Analysis of Unstable Phenomena in Premixed Flame Burners and their Active Control

A. Koichi Hayashi[1], Hiroyuki Sato[1], Takashi Endo[1], Yoshikatsu Yasunami[1], Shuichi Yoshimi[1], Satoru Ogawa[2], Masaru Ikame[3], Takeyuki Kishi[3], Katsuhide Hiraoka[3], Kazuyoshi Harumi[3], and Hideyuki Oka[3]

[1] Aoyama Gakuin University, 6-16-1 Chitosedai, Setagaya-ku, Tokyo 157-8572, Japan
[2] National Aerospace Laboratory, 7-44-1, Jindaiji-Higashi, Chofu, Tokyo 182-8522, Japan
[3] National Maritime research Institute, 6-38-1 Shinkawa, Mitaka, Tokyo 181-0004, Jpan

Abstract

A premixed swirled burner system with methane and air is studied concerning its stable and unstable mode and developing its feedback control system. The secondary fuel and oxidizer injection system as well as speaker are used as actuator and a microphone and pressure gauge are used as sensors. Using H2 control analysis, the swirled burner is successfully controlled.

1. Introduction

An extensive review on combustion dynamics and control was performed by Candel[1] to give its future direction. He pointed out that prediction of instability, LES and DNS for instability simulation, rational analysis for real system, sensors, actuators, and control algorithms must be studied and developed.

There are three key issues to study combustion control; sound (acoustics), heat release (combustion), and vortex (fluid dynamics). Furthermore their coupled factors must also be investigated such as sound-heat release, heat release-vortex, and vortex-sound, where its system is shown in Eq. 1. First we have to analyze relations between instability and three major causes and coupled terms independently. To analyze such problem there are three methods to apply; experimental approach, analytical approach, and numerical approach. Each method is necessary to be set up to elucidate and to develop active control system for flame instability.

$$\frac{d^2 p'}{dt^2} + a\frac{dp'}{dt} + bp' = F_{sound}(t,t_s) + F_{heat\ release}(t,t_{hr}) + F_{vortices}(t,t_v) + coupling\quad terms \tag{1}$$

Historically many researchers have been working on active combustion control (ACC). Studies of oscillatory combustion have been carried out extensively. In past investigations, general considerations of oscillatory phenomena were investigated mainly. However, in these days, ACC of the oscillatory flame has a lot of attention as a technical method of clean combustion to reduce its pollutions. Several studies succeeded at the application of active combustion control meant to suppress longitudinal mode oscillations in laboratory scale combustors [e.g., 2-4]. In these cases, systems have used various means of actuation like loudspeakers, fuel-flow modulation, and so on. In recent concerns about the ACC, development of the control system to achieve real time observation is a key point of ACC investigation. Furthermore, the important point is to consider delay times caused by the period of input and output signals with a control theory. Under these circumstances, Zinn and coworkers [e.g., 5-7] were investigated the ACC strenuously for gas turbine combustor. Contents of their researches are the experiment, numerical simulation, and furthermore theoretical analysis. Candel and coworkers are also one of the ACC research group, and they carried out an experimental study based on adaptive control algorithms [8]. Ghoniem and coworkers investigated the ACC with theoretical and numerical analyses [9]. In their papers, it is proposed that developing the models for the acoustics, the heat-release dynamics, their coupling, and fluid dynamics is physically based.

The whole system of study is shown in Table 1 where three factors and three methods are listed and the present study is marked by circles. The present study covers three regions; sound-active control (Open loop) and -active control (Closed loop) and heat release-active control (Open loop). In both cases of sound and heat release, microphone is used as a sensor. NOx sensor is demonstrated as a preliminary measurement. The final purpose is to control noise, emissions, and combustion efficiency.

Table 1 Research matrix for control combustion

	Experiment		Analysis	Numerical Simulation
	Active Control Open loop	Active Control Closed loop		
Sound: Sensor-microphone -pressure gauge Actuator-speaker	○	○	x	x
Heat Release Sensor-microphone Actuator-injector	○	x	x	x
Vortices	x	x	x	x

2. Experimental and control systems

Figure 1 shows schematics of premixed combustor and swirl-type flame holder. Size of combustor is 150×150×300 (mm), and the diameter of swirl-type nozzle is 30 mm. The nozzle has twelve vanes and its angle ? is 45 degrees. Pure CH_4 gas was used as a fuel and it was premixed with air before the ignition.

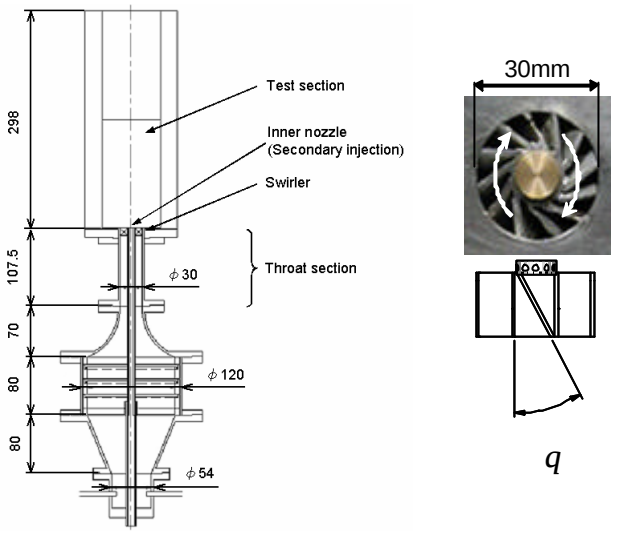

Fig. 1 Schematics of combustor and swirl-type flame holder

As a control system, microphone and loudspeaker were equipped for a sensor and actuator. To control the gain of loudspeaker, MATLAB/Simlink and dSPACE units were installed in the ACC system. The active control algorithm was based on the H2 control method using modal analysis. This is for the feedback control system and its purpose is to reduce the order of developed controller. To develop a controller with minimum order, active real time observation will be possible.

3. Control algorithm

In this section a feedback acoustic control based on mode analysis is discussed to set up a closed loop feedback control system for our swirl burner.

3.1 Structure-acoustics identification by experimental mode analysis

Structure-acoustics mode kinetic equation is described by the following;

$$m\ddot{x} + c\dot{x} + kx = B_{2,e}u \tag{2}$$

where x is a displacement vector, m, c, k are mass matrix of the system, damping matrix, stiffness matrix,

respectively. $B_{2,e}$, u are control input matrix and input for acoustic control, respectively. Furthermore output for structural oscillation and sound pressure are described as follows;

$$y = C_0 q_0 \tag{3}$$

where $q = (x^T, \dot{x}^T)^T$, C_0 is observation output.

Performing a oscillation experiment as the input from control sound source, frequency response function of structure-acoustics mode. If sound source is considered to come from a flame holder region, it must be necessary to count on a time delay between speaker and microphone. Besides a computational time delay of digital controller exists as a waste time in acoustic control system. Hence the following equations are considered as such waste time factor;

$$G_t(jw) = e^{-t(jw)} \tag{4}$$

$$T = L / a \tag{5}$$

where G_t is waste time factor, L a distance from speaker to microphone, T a delay time, and a speed of sound.

If G_0 is the transfer function corrected by phase shift, the transfer function measured experimentally is

$$G_m(jw) = G_0(jw) \cdot G_t(jw) \tag{6}$$

From Eq. 6

$$G_0(jw) = \frac{G_m(jw)}{G_t(jw)} \tag{7}$$

The control system is designed by using a model combined identified transfer function model with the waste time factor. This identification is shown in Fig. 2. The phase falls off before the correction is effectively improved by considering the waste time.

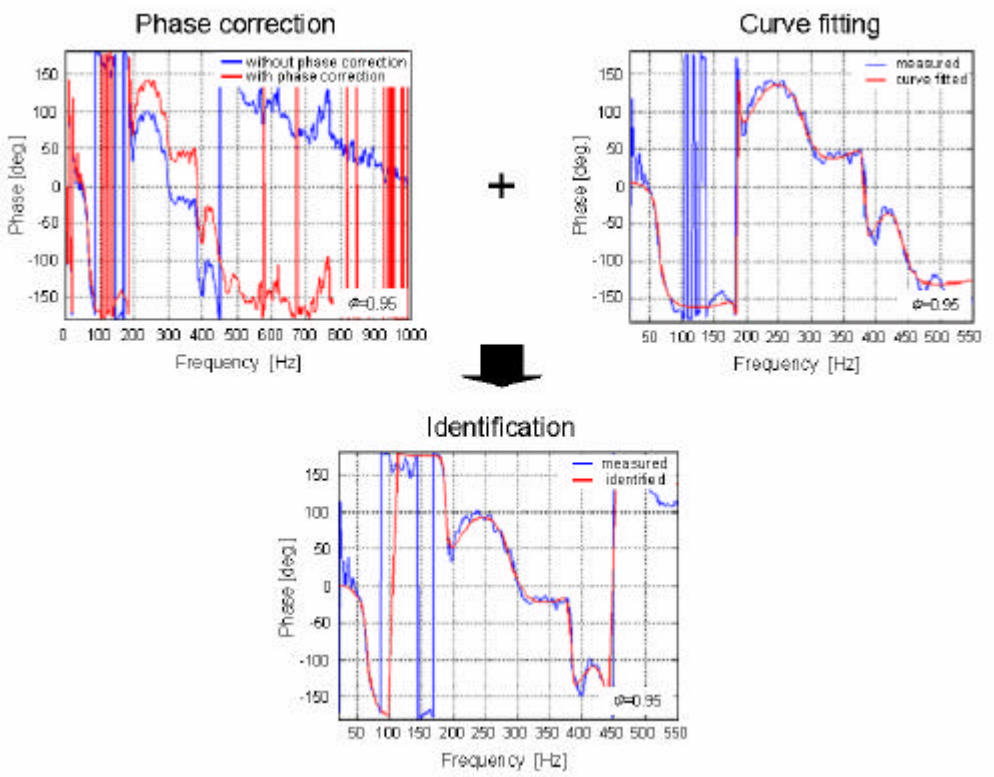

Fig. 2 Identification of the present transfer function

To Eq. 6, where the waste time is taken account in the transfer function, if the transfer function G_m is

that with a general viscous fall off, G_m becomes using the transfer function G with viscous damping and without waste time as follows:

$$G_m(jw) = G_0(jw) \cdot G(jw) \tag{8}$$

where we must know the difference between Eqs. 6 and 8.

G in Eq. 8 is described as follows:

$$G(jw) = \sum_{r=1}^{n} \left\{ \frac{U_r + jV_r}{j(w - w_r) + s_r} + \frac{U_r - jV_r}{j(w + w_r) + s_r} \right\} \tag{9}$$

where w_r and s_r are the damping eigen angular frequency and mode damping rate, respectively and U_r and V_r are the mode constant for the general viscous damping.

If we take

$$a_r = s_r^2 + w_r^2 \tag{10}$$

$$b_r = 2s_r \tag{11}$$

$$g_r = 2(s_r U_r - w_r V_r) \tag{12}$$

$$h_r = 2U_r \quad , \tag{13}$$

where Eq. 10 is the zero order coefficient of the denominator for r-order, Eq. 11 the first order coefficient of the denominator for r-order, Eq. 12 the zero order coefficient of the numerator for r-order, and Eq. 13 the first order coefficient of the numerator for r-order. For $s = jw$ Eq. 9 becomes with Eqs. 10 through 13 as follows:

$$G(s) = \sum_{r=1}^{n} \left\{ \frac{h_r s + g_r}{s^2 + b_r s + a_r} \right\} \tag{14}$$

Since the transfer function G_m measured for Eq. 8 and the transfer function G_0 corrected its phase delay are known, for G(s) of Eq. 14 the mode characteristics in Eq. 10 through 13 are identified by the variation iteration method with a curve fit for transfer functions where the sound is reduced best.

Based on the controllable conical form, Equation 2 is transferred to the equation of states and the out put equation. When the mode axis $x = [x_1, x_2, \cdots, x_n]^T$ of r-order is applied,

$$\begin{aligned} \dot{q}_{e,r} &= A_{e,r} q_{e,r} + B_{2e,r} u \\ &= \begin{bmatrix} 0 & -b_r \\ 1 & -a_r \end{bmatrix} \begin{Bmatrix} x_r \\ \dot{x}_r \end{Bmatrix} + \begin{bmatrix} g_r \\ h_r \end{bmatrix} u \end{aligned} \tag{15}$$

$$\begin{aligned} y_r &= C_{e,r} q_{e,r} \\ &= [0 \quad 1] q_{e,r} \end{aligned} \tag{16}$$

3.2 Active control algorithm

In this investigation, the acoustic control for a mixed sensibility problem is considered as shown in Fig. 3. *G*(*s*) is the control object of the structure-acoustics system, *K*(*s*) the controller, Z_{21} and Z_{22} the noise reduction performance and control amount for robust stability, respectively. W_1 and W_2 show the weighting function of frequency and are descried as follows:

$$W_i(s) = \begin{pmatrix} A_{wi} & B_{wi} \\ C_{wi} & D_{wi} \end{pmatrix} \tag{17}$$

y means the output signal of microphone, and it is used as a feedback signal for the control system. As for the system, the noise reduction performance and the robust stability are evaluated by the sensitivity function, *S*(*s*) about between a disturbance, *w* and a deviation, *e* and the complementary sensitivity function, *T*(*s*) related to the output, y. These function are described as follows:

$$S(s)=\frac{1}{1+G(s)K(s)} \quad , \quad T(s)=\frac{G(s)K(s)}{1+G(s)K(s)} \tag{18}$$

When the system is controlled primarily by the resonance peak of an acoustic transfer function based on the sensitivity function, $S(s)$, detailed analysis to configure the frequency weighting is required by Eq. (17). In that case, since an enhancement of control order is caused by the detailed frequency weighting, it has a problem to develop the real-time control. Thus, the control system shown in Fig. 4 is conceived. In the block diagram, w_d and w_s are the distributions due to an external sound source and a noise of sensor, respectively. As for the performance function of noise reduction, the transfer function $S_p(s)$ related to the loop between the disturbance, w_d and the output, y is taken by

$$S_p(s)=\frac{G(s)}{1+G(s)K(s)} \quad . \tag{19}$$

This equation is the sensitivity function expressed by $G(s)K(s)$, which is classified by the plant characteristics, $G(s)$. The function $S_p(s)$ is suitable for the evaluation of acoustic level at a resonance in a stricture-acoustic coupled system. Furthermore, it seems that the function takes an advantage when the frequency weighting function and mode weighting are combined for the frequency fairing.

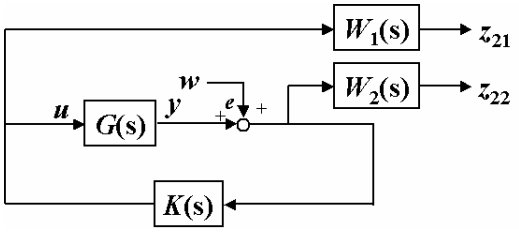

Fig. 3 Acoustic control for a mixed sensibility

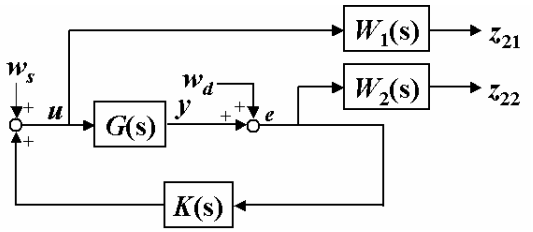

Fig. 4 Acoustic control with external sound and Sensor noise

According to the method of frequency fairing which combined the frequency weighting function and mode weighting, detailed frequency fairing held the increase of control order becomes possible due to the performance of Z_{21} descried by the frequency weighting function W_1 and the mode weighting for the noise efficiency and that of Z_{22} defined by the amount of W_2 for the robust stability. Then, the output equation shown in Eq. (16) is rewritten as follows:

$$\begin{aligned} y_{w,r} &= C_{e,r} q_{ew,r} = \begin{bmatrix} 0 & 1 \end{bmatrix} \begin{pmatrix} w_r x_r \\ \dot{w_r x_r} \end{pmatrix} \\ &= C_{ew,r} q_{e,r} = \begin{bmatrix} 0 & w_r \end{bmatrix} \begin{pmatrix} x_r \\ \dot{x}_r \end{pmatrix} \end{aligned} \tag{20}$$

where w_r is the mode weighting.

In summary, the equations of state for a plant considered the frequency fairing is expressed by

$$\begin{aligned} G: &\quad \dot{q} = Aq + Bu \\ &\quad y = Cq + Du \\ W_1: &\quad \dot{q}_1 = A_1 q_1 + B_1 u \\ &\quad Z_{21} = C_1 q_1 + D_1 u \\ W_2: &\quad \dot{q}_2 = A_2 q_2 + B_2 (w + y) \\ &\quad Z_{22} = C_2 q_2 + D_2 (w + y) \end{aligned} \tag{21}$$

The expression with matrix is

$$\dot{q} = \begin{bmatrix} A & 0 & 0 \\ 0 & A_1 & 0 \\ B_2C & 0 & A_2 \end{bmatrix} q + \begin{bmatrix} 0 & B \\ 0 & B_1 \\ B_2 & B_2D \end{bmatrix} \begin{pmatrix} w \\ u \end{pmatrix}$$
$$\begin{pmatrix} Z_{21} \\ Z_{22} \\ y \end{pmatrix} = \begin{bmatrix} C & 0 & 0 \\ 0 & C_1 & 0 \\ D_2C & 0 & C_2 \end{bmatrix} q + \begin{bmatrix} 0 & D \\ 0 & D_1 \\ D_2 & D_2D \end{bmatrix} \begin{pmatrix} w \\ u \end{pmatrix} \quad (22)$$

Designing a controller, we can provided disturbances to the system input, but these disturbances work well to the equivalence ration which is applied for the system design and do not work to diverge to the system when the peak of transfer function are shifted. Hence considering that the disturbance is located to the system output as shown in Fig.3, the design of controller which can response well to the change of equivalence rations by defining the frequency weighting function to the disturbance with a band path filter.

Actually we use H2 control theory at this moment. In other words, we design a controller K which minimizes the H2 norm from w to Z_{22}. In this case, the evaluation function J is;

$$J = \int_0^\infty \left(u^T W_1 u + x^T W_2 x \right) dt \quad (23)$$

where the first term of RHS is oscillating energy and the second term in the control energy.

After solving the optimum problem for the evaluation function J and getting the optimum values of variable matrixes A, B, C, D, the controller $K(s)$ is fixed.

4. Results and discussion

In order to understand the characteristics of the swirled flame burner, combustion characteristic maps are developed for three swirl angles of 15, 30, and 45 degrees, methane flow rates between 1.5 and 2.5 litters/min, and the equivalence ratios from 0 to 2.0. Figure 5 shows the combustion characteristic map of 45 degrees swirl angle, where Fig. 5-(a) is the case of without an upstream extension tube and Fig. 5-(b) is that of with an upstream extension tube. Oscillatory combustion occurs when the methane flow rate ranges from 1.50 l/min to 2.50 l/min in both fuel-rich and -lean conditions. Oscillatory flames characterized by basically fuel-rich conditions are defined by Type-A and that by fuel-lean conditions are by Type-B. Type-A flame is held at the outer rim of the swirled burner and Type-B is stabilized at the inner rim. From the map we can recognize which way the flame becomes stable or unstable by changing the main flow rate or equivalence ratio. When the mixture temperature increases, blow off conditions become lower at equivalence ratios.

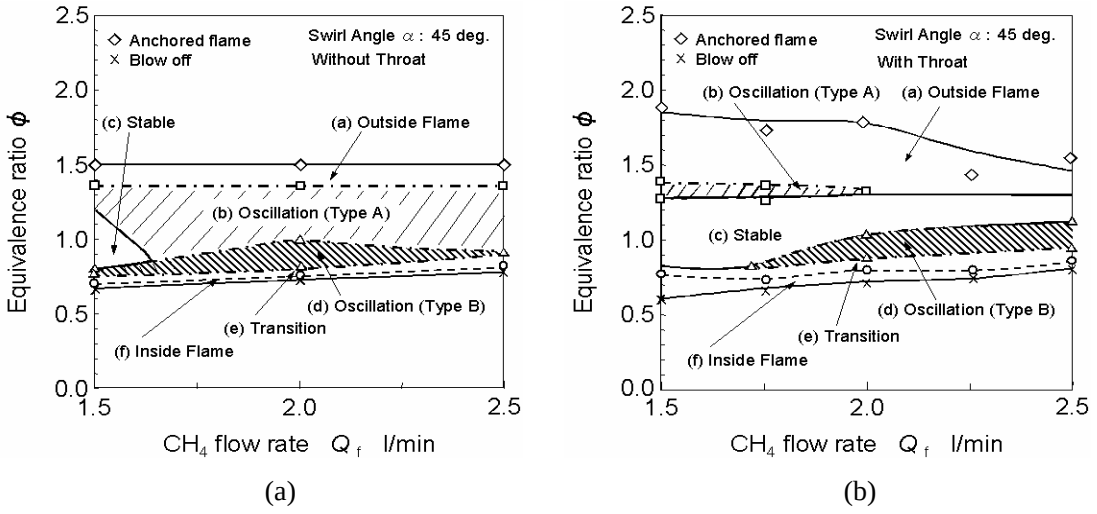

(a) (b)

Fig. 5 Combustion characteristic map: (a) without extension tube and (b) with extension tube.

4.1 Sound (acoustics)

Acoustics is one of major problem for many industry applications. A microphone as a sensor and speaker as an actuator are used for active control to elucidate such unstable problem with acoustics. Passive control system using microphone and speaker is spared in the present report since it has been reported last year.

4.1.1 Inlet conditions for resonant noise problem with FFT analysis

A tube from a mixing point of fuel and oxidizer to burner provide a Helmholtz-type resonance for a longitudinal mode. A short tube and long tube which is 100 mm longer than the short one are used to study the resonance problem. Both tube diameter are the same as 30 mm.

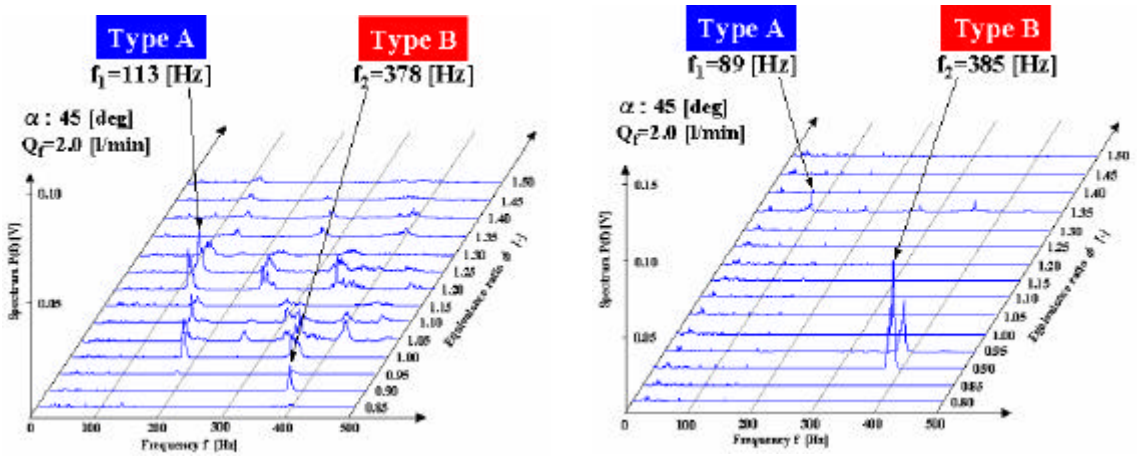

(a) (b)

Fig. 6 FFT spectra of noise (a) without additional inlet tube and (b) with additional inlet tube

As shown in Fig. 6, the additional inlet tube provides a smoother noise spectra in combustion chamber where Type B frequency of around 380 Hz is Helmholtz type resonance based on the longitudinal combustion chamber size, which corresponds to acoustic speed divided by one quarter of chamber size.

From these results we can see, but do not confirm yet, that the source of combustion noise comes from the edge of the burner due to fluid dynamics instability.

4.1.2 Closed feedback control for noise reduction using a speaker

A closed loop feedback control system is performed based on the control analysis before-mentioned. Figure 7 shows the acoustic pressure to time after the closed loop feedback control system is applied for speaker actuation. At the time of 10 sec the speaker is activated to reduce noise up to about 30 %. Since

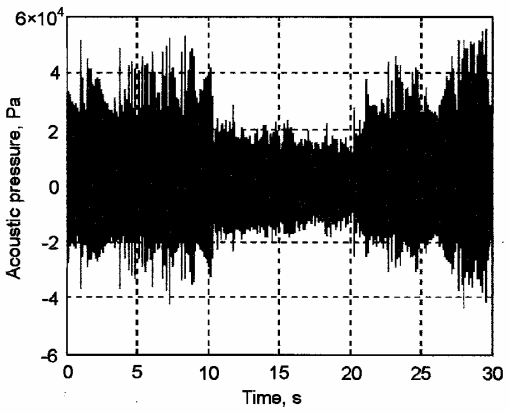

Fig. 7 Acoustic pressure in the system with the feedback control;
Time between 10 and 20 sec are the sequence of feedback control.

speaker is used, the control time delay is very short (about 1msec) in this case. After making the control off, the acoustic pressure comes back to the original noise level at the time of 20 sec.

Figure 8 is the sound pressure (noise) profiles to acoustic frequency to show several resonant frequencies. The dark curve is the case of feedback controlling the system and the weak color curve is the non-control case. Apparently the noise levels are reduced through the developed control system which is described in Section 3.

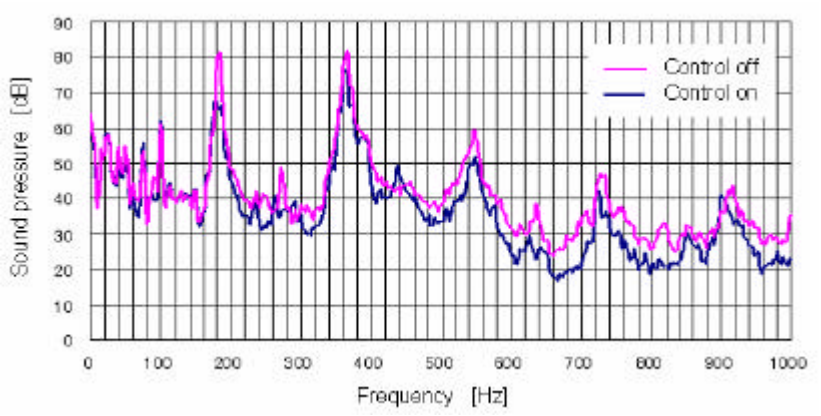

Fig. 8 Sound pressure profiles to noise frequency at the feedback control.

4.2 Control by secondary injection of oxidizer or fuel (heat release)

The control by the secondary injection is performed using a nozzle with 12 holes of 1mm in diameter toward 12 swirler blades as shown in Fig. 1. Air or methane are used as the secondary gas. The injection direction is the tangential to the main swirled flow to provide a good mixing with the main mixture flow.

4.2.1 The effect of the secondary injection to noise: air case and methane case.

The purpose and results are different between when air is used as a secondary injection and when methane is used for that. However in the present case, where the equivalence ratio is close to the stoichiometric, the results for both cases are more or less the same. Figure 9 is the case of noise reduction using air: the top figure is the case of without air secondary injection and the bottom one is that with air secondary injection. We could recognize that the noise of the system, especially the Helmholtz-type

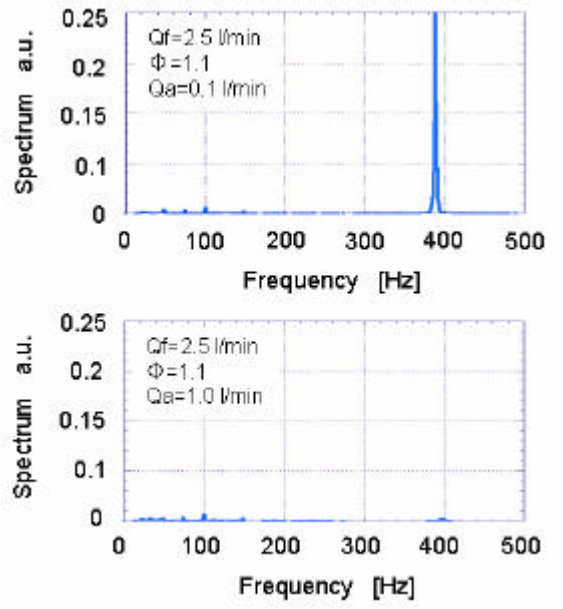

Fig. 9 The case of secondary injection by air

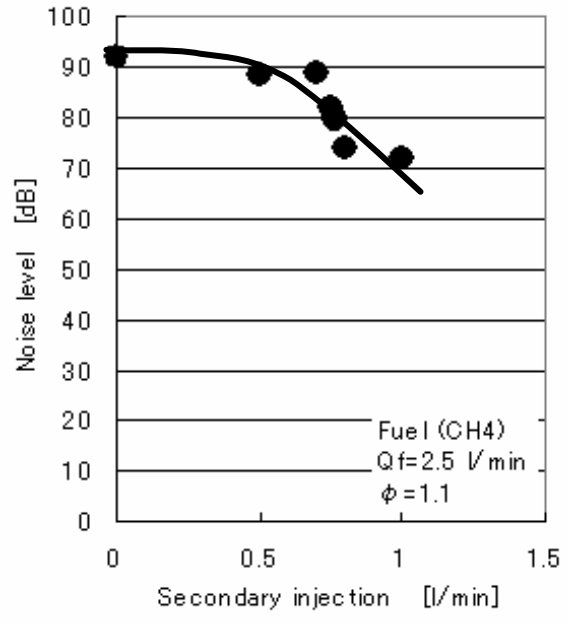

Fig. 10 The case of secondary injection by methane

resonant noise disappeared. Figure 10 shows the case of noise reduction with methane. The main mixture is a bit rich (ϕ=1.1) but the system noise is reduced with the methane secondary injection. In this case the combustion system get more heat release to be stable.

4.3 Effect of secondary injection to emissions

NOx and CO are measured to see the effect of secondary injection of methane to the present system. The results are that when air or methane is injected, both NOx and CO are reduced; i.e., in the present condition such injection reduce emissions. We have to study the sensitivity of injection to reduce emission. Figure 11 is the case of air secondary injection and Fig. 12 is the case of methane.

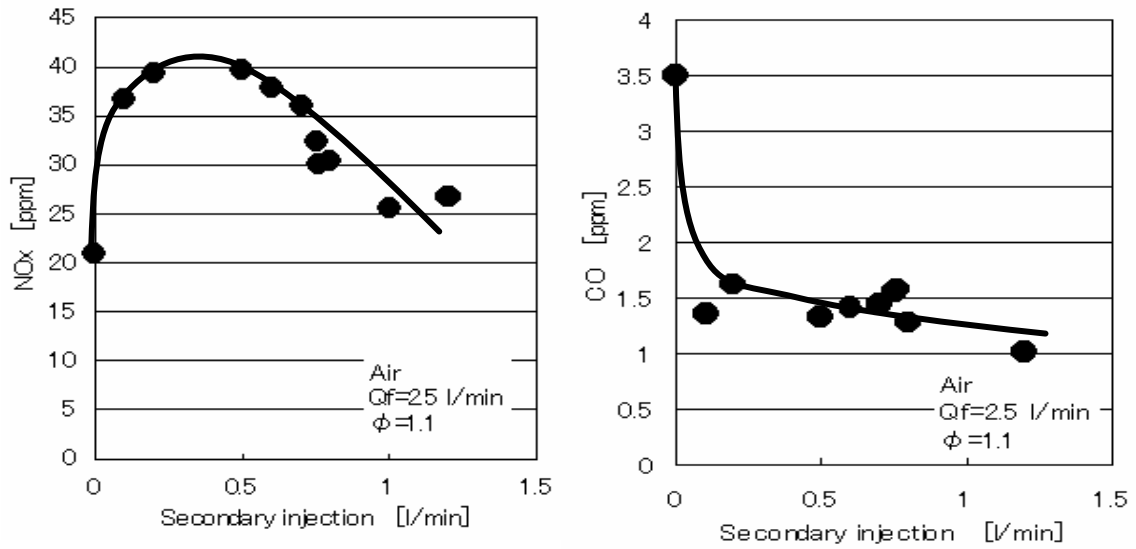

Fig. 11 The effect of air secondary injection to emission of NOx and CO

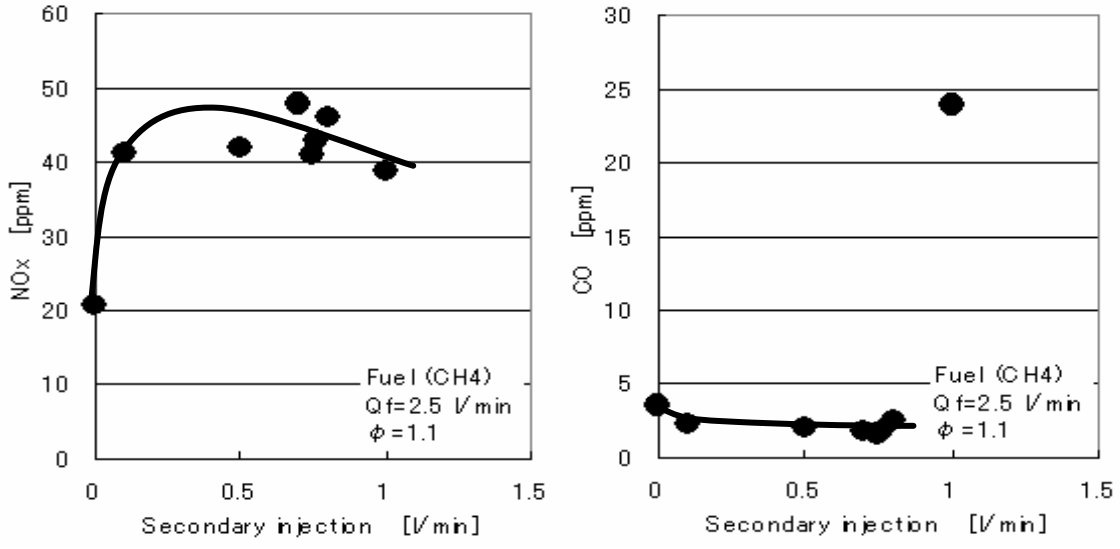

Fig. 12 The effect of methane secondary injection to emission of NOx and CO

4.4 New actuator for the secondary injection system (National Maritime Research Institute)

Piezo-ceramic type actuator is used to reduce noise for the combustible case and non-combustible case. The use of this actuator provides a large amount of secondary injection with less time delay. A preliminary results show that at the 400 Hz actuation frequency both cases have the same level of noise.

This implies that in this case 400 Hz actuation is the boundary of fluid dynamic noise; i.e., the fulid dynamic noise becomes the same level as the noise of combustion and fluid dynamics.

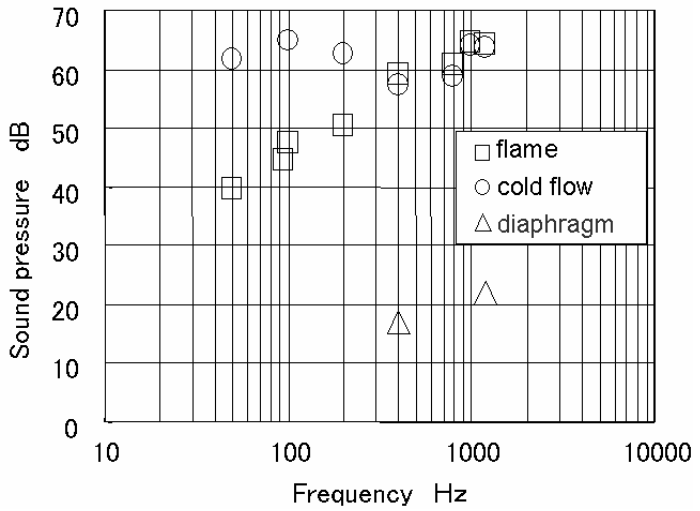

Fig. 13 A comparison of noise level between combustion case and non-combustion case.

Concluding remarks

The swirled burner with air/methane premixed flames was studied at the aspect of stable and unstable modes. The characteristic map was obtained to elucidate such instability mode to establish a control system. With the fundamental study the H2 control ayatem was applied to control the swirled burner combustion system and gave a successful feedback control for noise. The future study includes a development of analytical and numerical systems for control combustion and new types of sensors and actuators.

References

1. Candel, S., 29th Int. Symp. on Combustion, July 20-26, 2002
2. Bloxsidge, G. J., Dowling, A. P., Hooper, N, and Langhorne, P. J., *AIAA J.*, vol. 26, no. 7, pp. 783, 1988
1. Lang, W., Poinsot, T., and Candel, S., *Combustion and Flame*: 70, pp.281, 1987
2. Gulati, A, and Mani, R, *Journal of Propulsion and Power*, vol. 8, no. 5, pp. 1109, 1992
3. Neumeier, Y., and Zinn, B. T., *AIAA Paper* 96-0758, 1996
4. Lieuwen, T. C., and Zinn, B. T., *AIAA Paper* 98-0641, 1998
5. Lieuwen, T. C., and Zinn, B. T., *AIAA Paper* 2000-0707, 2000
6. Mettenleiter, M., Haile, E., and Candel, S., *Journal of Sound and Vibration*, 230(4), pp.761-789, 2000
7. Hathout, J. P., Fleifil, M., Annaswamy, A. M., and Ghoniem, A. F., *Journal of Propulsion and Power*, vol. 18, no. 2, pp. 390, 2002